

# Development Status of the Nonambipolar Electron Source

Ben Longmier<sup>\*</sup> and Noah Hershkowitz<sup>†</sup>  
*University of Wisconsin - Madison, Madison, WI 53706*

**A Radio Frequency (rf) plasma-based electron source that does not rely on electron emission at a cathode surface has been constructed. All of the random electron flux incident on an exit aperture is extracted through an electron sheath resulting in total nonambipolar flow within the device when the ratio of the ion loss area to the electron loss area is approximately equal to the square-root of the ratio of the ion mass to the electron mass, and the ion sheath potential drop at the chamber walls is much larger than  $T_e/e$ . The Non-ambipolar Electron Source (NES) has an axisymmetric magnetic field of up to 275 Gauss at the extraction aperture that results in a uniform plasma potential across the aperture, allowing the extraction of all the incident electron flux without the use of grids. A prototype NES has produced 30 A of continuous electron current, using 2 sccm Xe, 1300 W rf power at 13.56 MHz, yielding a 180x gas utilization factor. A helicon mode transition has also been identified during NES operation with an argon feed gas, using 15 sccm Ar, 1000 W RF, and 100 gauss magnetic field.**

---

<sup>\*</sup> Graduate Student, Engineering Physics Department, 1500 Engineering Dr., Madison WI 53706, AIAA Member.

<sup>†</sup> Professor, Engineering Physics Department, 1500 Engineering Dr., Madison WI 53706.

## I. Introduction

Hollow cathodes are used in a variety of industrial applications<sup>1-5</sup> and are currently used as plasma and electron sources onboard spacecraft that employ ion thruster technology. Hollow cathodes have a finite lifetime, due largely to cathode deterioration, contamination, and barium diffusion rates.<sup>6</sup> This is usually not a problem for industrial applications however it can be a critical problem for spacecraft that use hollow cathode electron sources in a plasma generation stage or in a neutralization stage of an ion thruster, where long-duration continuous thrust missions require an electron source with lifetimes in excess of the mission duration.<sup>7</sup> While using ion propulsion for longer duration missions is beneficial because of fuel, mass, and time savings (as opposed to impulsive chemical rocket burns), the lifetime of some operating components for ion propulsion systems, such as the hollow cathode source, may be limited to 3-4 years,<sup>7-9</sup> thereby making longer continuous-thrust missions infeasible.

In gridded ion propulsion systems plasma is initially generated by energetic electrons from a hollow cathode and ions are extracted and accelerated by a series of differentially biased grids. The positive beam of ions is later neutralized with a stream of electrons that are introduced downstream of the ion acceleration grids by a second hollow cathode. Similarly, Hall thrusters use hollow cathodes as a source of plasma and as a source of electrons for neutralizing the accelerated ion beam. Traditionally, hollow cathode sources employing inserts with a refractory metal and a barium oxide-calcium oxide-aluminum oxide coating have been used as neutralizing sources on spacecraft because of their low work function, high electron current density, and relatively low power requirements.<sup>9</sup> In general, hollow cathode discharges are known as relatively efficient ion, electron, and plasma sources where dense plasma is formed interior to a hollow cylindrical cavity. Ion sheaths form along the cavity walls and act to reflect and confine electrons in the bulk plasma. The electrostatic confinement of electrons leads to an efficient ionization of the working gas. An electron sheath (a sheath where ion density can be neglected) forms across the exit aperture of hollow cathodes, acting to extract all or most incident electrons and to reflect all ions. In this way, there is a strong non-ambipolar flow of electrons and ions with all of the electrons leaving the plasma through the aperture and all of the ions leaving the plasma at the cavity wall.

Radio frequency (RF) generated plasmas are attractive as electron sources as replacements to hollow cathodes for industrial plasma applications and electric propulsion devices because electron generation does not depend on cathode materials and they provide high ionization efficiency and long life operation. In this way, rf plasma sources provide an alternative approach to electron generation that does not consume electrode material while providing electrons, thereby allowing for high purity operation in industrial applications and for longer operational lifetimes in spacecraft thruster components. A variety of rf sources exist including capacitive and inductive sources,<sup>10, 11</sup> which can operate without magnetic fields, and both electron cyclotron resonance (ECR) and helicon sources, which require magnetic fields.<sup>12</sup> Helicon sources appear to be the best choice of rf plasma sources for use in high power/current ion propulsion because they have the highest ionization efficiency and can produce the highest plasma densities, up to  $10^{13} \text{ cm}^{-3}$  is common<sup>13</sup>, for a given rf power. The magnetic fields that are required for ECR and helicon plasma sources can be generated by electromagnets or permanent magnets. If insufficient rf power is available, helicon sources operate as inductive sources resulting in decreased plasma densities. At much lower rf powers, the plasma is capacitively coupled with even lower plasma densities.

ECR plasma sources have previously been used as a source of electrons for neutralizing gridded ion thrusters.<sup>14, 15</sup> Microwave sources without applied magnetic fields have also been proposed for spacecraft neutralizer applications.<sup>16, 17</sup> While efficient at plasma production, these devices to date have produced less than 2.5 A of electron beam current,<sup>15-18</sup> limiting their usefulness in higher current and higher thrust applications.

Experiments with the Phaedrus tandem mirror device<sup>19</sup> showed that the radial plasma potential interior to a magnetic flux tube can be controlled with an annular ring in the presence of an axial magnetic field. The non-intuitive result from that experiment is that the potential of the ring determines the plasma potential for radii less than the radius of the ring. This result indicated the possibility of plasma potential control at a boundary.

The current proof of principle device at the University of Wisconsin-Madison has produced a plasma with densities from  $10^{10} \text{ cm}^{-3}$  to  $3 \times 10^{13} \text{ cm}^{-3}$ , and 30 A of electron current. The electron current was extracted through an electron sheath (sheath where ion density can be neglected) near a grounded ring located at the plasma source boundary, with a 275 gauss axially symmetric magnetic field.

This Non-ambipolar Electron Source (NES) operates with all of the electron current extracted at the ring and all of the ion current extracted to its walls. Initial work<sup>20, 21</sup> was funded as part of NASA's HiPEP program<sup>22</sup> to develop a high powered long duration ion propulsion system in support of the JIMO mission. In addition to achieving high

electron current output, NES achieved gas utilization factors as high as 180, compared to gas utilization factors of 4 for current ECR electron sources.<sup>23</sup> This NES technology has the ability to enable high power cargo transfer missions to the moon or Mars<sup>24-26</sup> while eliminating one of the lifetime restrictions that many electric propulsion devices have previously been faced with.

This paper discusses further improvements to the operation of NES as an rf plasma electron source for the purposes of plasma generation or neutralization in a Hall or gridded ion thruster.

## II. Experimental Hardware

The hardware used in this experiment contains: a Non-ambipolar Electron Source, made up of an ion collection cylinder, electron extraction ring, rf antenna, Faraday shield, and an electromagnet; a vacuum chamber; a Langmuir probe / anode and an emissive probe; and argon feed gas. A schematic illustration of the plasma chamber containing NES and supporting vacuum hardware is shown in Fig. 1 and a 3D CAD drawing of NES and supporting vacuum hardware is shown in Fig. 2.

### A. NES

A 6.0 cm I.D., 7 cm O.D., 21cm long, hollow graphite cylinder is located coaxially within the vacuum chamber as the ion collection cylinder and can be biased from 0 to -100 V. This cylinder is a radial boundary for the plasma and acts as a location for the formation of an ion sheath that prevents electrons from leaking to the chamber walls. The ion collection cylinder also has 8 axial slots (1 mm wide), which allow the dB/dt fields into the plasma but limit the dE/dt fields,<sup>27</sup> effectively serving as a Faraday shield for the plasma within NES. The electron extraction ring is an electrically grounded 1.25 cm dia. graphite ring that sits inside an insulating boron nitride disk. This grounded ring combined with the magnetic field creates an electron sheath, uniform across the area of the ring, limiting the ion flow, and gives a potential reference for the plasma near 0 to +5 V. The rf antenna is formed from a single turn ¼” water cooled copper pipe and operates at power levels up to 1200 W at an rf frequency of 13.56 MHz. The magnet coil geometry is discussed below and illustrated in Fig 2.

### B. Vacuum chamber

The electron source is set within a 50 cm long 7.5 cm dia. quartz tube that is connected to a grounded vacuum tee. A 4” diffusion pump with a cold trap creates a base vacuum pressure of  $5 \times 10^{-7}$  Torr.

### C. Diagnostic tools

A 0.1 mm dia. Tungsten emissive probe (not shown) is inserted from the right side of the chamber, see Fig. 1, and can be extended through the target side (right) of the plasma and into the source side (left), and is used to determine the plasma potential along the entire axis of the plume region and within NES. The emissive probe is operated in the limit of zero emission, resulting in increased accuracy of plasma potential measurements.<sup>28</sup> A double probe is used for plasma density measurements and is inserted from the left in Fig. 1

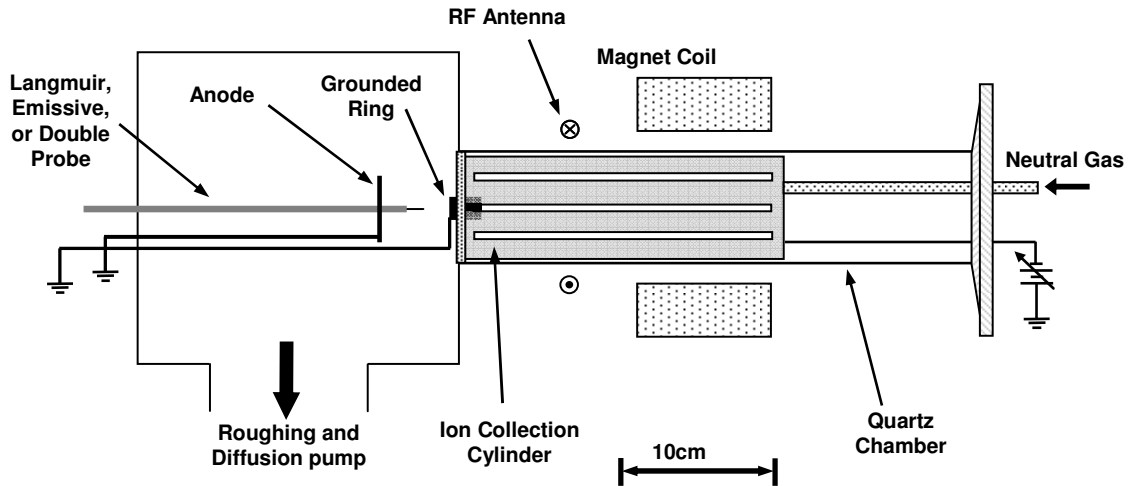


Figure 1. Schematic illustration of the plasma chamber containing the Nonambipolar Electron Source (NES) with supporting vacuum hardware and diagnostics.

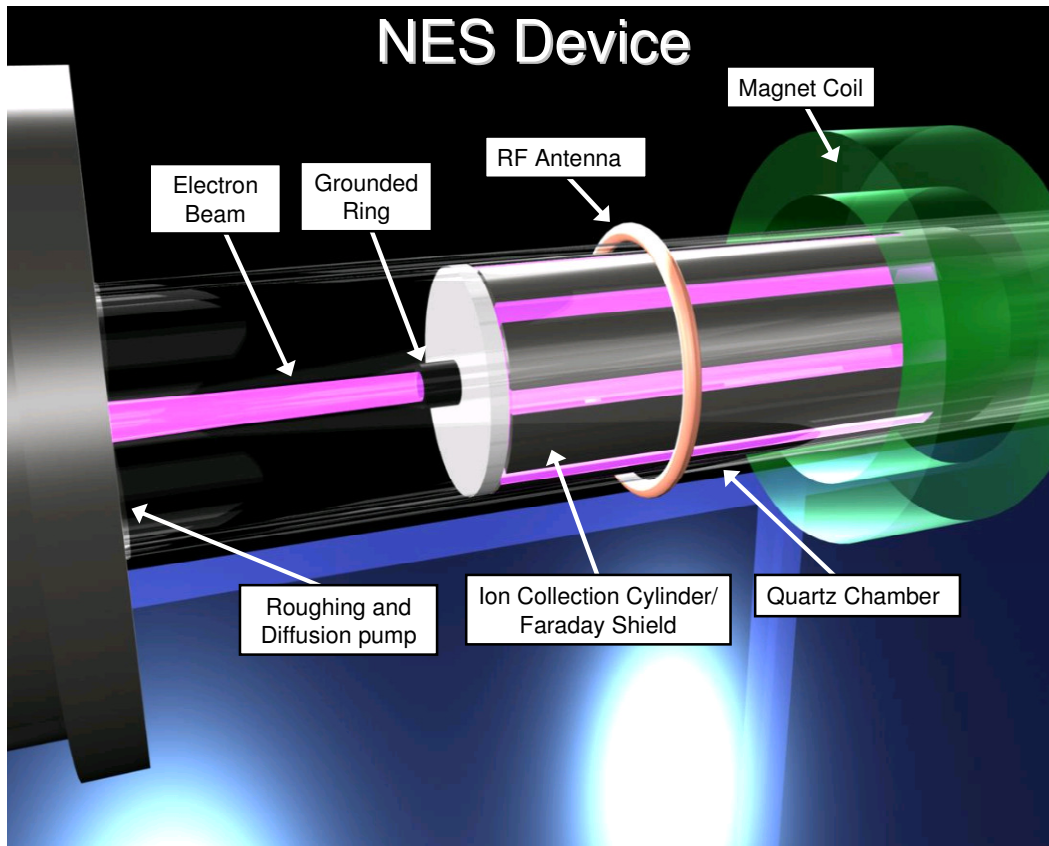


Figure 2. 3-D CAD illustration of the plasma chamber containing the Nonambipolar Electron Source (NES) with supporting vacuum hardware. NES is shifted to the right in this figure for visualization purposes.

#### D. Feed gas

Argon or xenon feed gas is introduced into the chamber from a mass flow controller (not shown) and flows into the source region where a plasma is excited by the rf antenna.

### E. Magnet geometry

An electromagnet has been used for all data presented in this paper and is especially useful for experiments that require varying magnetic field strengths, as seen in Fig. 3. Alternatively, a set of permanent magnets (Fig. 4a inset of chamber/magnet cross section) can be used to generate a solenoidal magnetic field in the axial direction of NES. These ferrite magnets have nearly a square cross section with the exception of a cylindrical void that allows space for the quartz chamber. The permanent magnets produce an expanding magnetic field in the region of the antenna and electron extraction ring similar in uniformity and shape to the electromagnet with the exception of a cusp, shown as point A in Fig 4b. Figure 4b is a plot of magnetic field lines for permanent magnets that can be used, created with FEMM 4.0. The dashed line in Fig. 4b defines where the magnetic field strength was sampled for Fig. 4a, where zero magnetic field strength is located at point A. The presence of a magnetic field not only makes higher density operation possible but the solenoidal magnetic field shape results in a uniform plasma

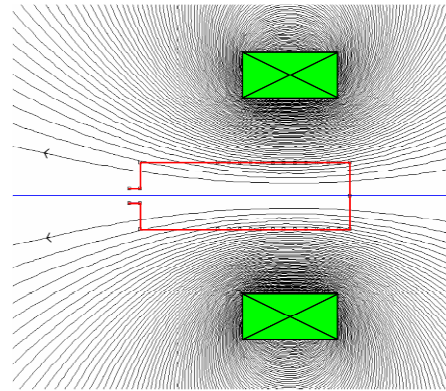


**Figure 3. Magnetic field lines for an axial cross section of the electromagnet used in NES.**

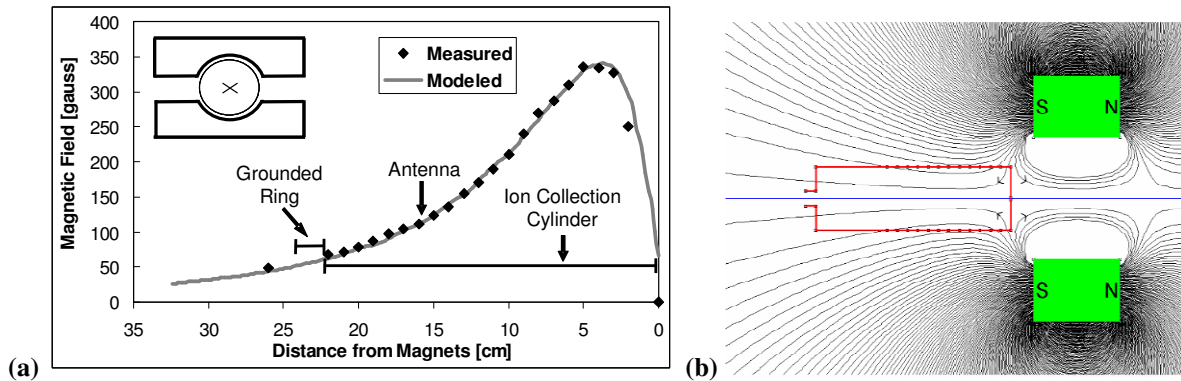


**Figure 4. Axial magnetic field strength from permanent magnets as a function of position. Transverse cross-section of magnets and quartz tube shown in inset (a), magnetic field lines for an axial cross section (b).**

potential across the exit aperture area. Similar results to the data presented in this paper were obtained with permanent magnets. Permanent magnets would be preferred for a flight version of an electron source because they do not require a power source for continual operation and are relatively light-weight compared to the coil and DC power source that would be required for an electromagnet.

### III. Experimental Results and Discussion

In order to maintain quasineutrality during steady state operation, the amount of electron loss from the plasma must be balanced by an equal amount of ion loss.<sup>29</sup> Neglecting secondary emission from ion-wall collisions, which is small, electrons and ions are born at an equal rate within the rf discharge and an efficient loss mechanism for the ions must be realized in order to extract an equal amount of electron current from the plasma source. Ultimately, plasma density and particle losses present the limiting factors for the total amount of electron current that can be extracted from the plasma for neutralizing an ion thruster.

It was previously demonstrated<sup>30</sup> that an electron sheath was responsible for the extraction of all random incident electron flux through an extraction aperture within NES. The amount of electron current that is extractable from NES is given by<sup>30</sup>

$$I_e = \frac{n_e e A_e \alpha_{e,e}}{4} \sqrt{\frac{8T_e}{\pi m_e}} \quad (1)$$

and the allowable ion loss area to electron loss area ratio is given by<sup>30</sup>

$$\frac{A_i}{A_e} \approx \sqrt{\frac{2m_i}{\pi m_e}} \quad (2)$$

Figure 5 shows a representative electron sheath within the NES device for a Xe plasma, where electron are extracted from the bulk (right) through the electron sheath (~ 2 cm) and through the electron extraction aperture to an external anode (0 cm). Similar to the electron sheaths within the DC chamber, the electron sheaths within the NES chamber exhibit a presheath of order  $T_e/2$  from the bulk region to the electron sheath. Similar electron sheath structures are observed in Ar plasmas, however the sheath amplitude is typically 16 V instead of 12 V for Xe. It is believed that additional ionization within the sheath region limits the amplitude of the electron sheath.

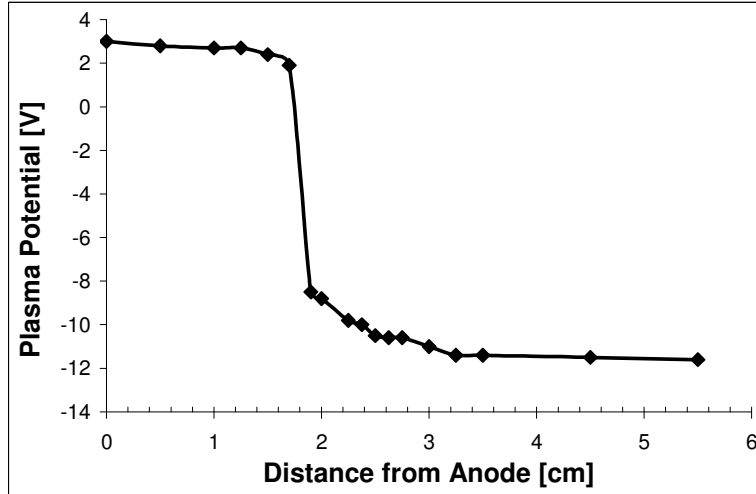


Figure 5. Typical axial plasma potential profile showing a ~12 V electron sheath in a Xe plasma within the NES device. Electrons are extracted from bulk plasma (right) through the extraction aperture (left).

### A. Improved Extraction Current and Plasma Density with Xenon

For a given rf power input and neutral gas pressure, xenon plasmas are observed to have a higher density than argon plasmas. This effect can be observed in Fig. 6 where plasma density is graphed as a function of the applied rf power for a xenon and an argon plasma with the same neutral gas pressure. It is believed that the difference in the ionization energies gives rise to the difference in plasma density, where argon's ionization energy is 15.75 eV and xenon's is 12.13 eV.<sup>31</sup> Figure 7 shows the plasma density as a function of the neutral gas pressure within NES as the pressure is varied from 0.5 mTorr to 12.5 mTorr. The xenon plasma has a consistently larger plasma density for any given neutral gas pressure compared to argon. The electron temperature within the discharges is

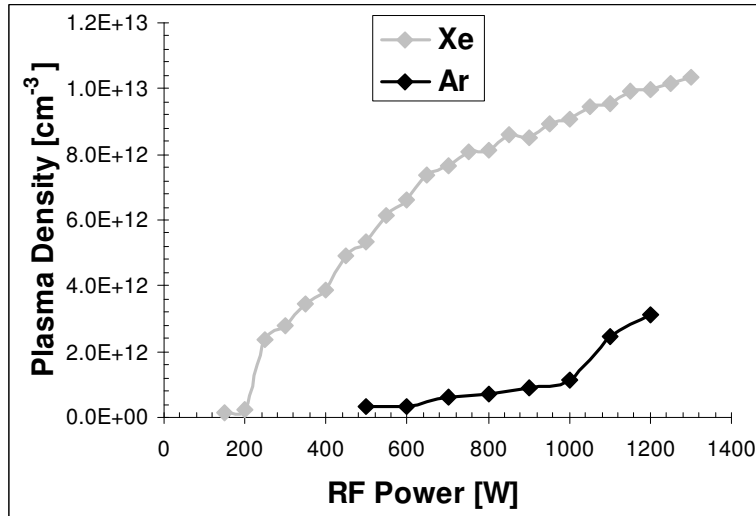
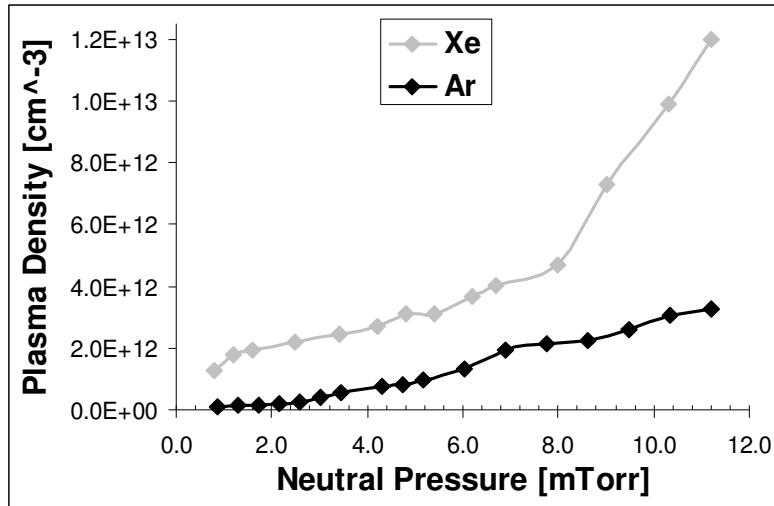


Figure 6. Argon and xenon plasma density as a function of the applied rf power. A radio frequency of 13.56 MHz was used with an applied DC magnetic field of 10 Gauss.

also similar when the two separate plasma discharges are compared at a given neutral gas pressure. Figure 8 shows the electron temperature within NES as a function of the neutral gas pressure for separate xenon and argon plasmas. For a given rf input power, 500 W for Figs. 7 and 8, the electron temperature of xenon and argon nearly overlap as the neutral pressure is varied from 0.5 to 12.5 mTorr within NES.

Previous argon plasma data<sup>30</sup> showed that a maximum of 15 A of electron extraction current was extracted from NES, however by using xenon as the neutral gas and identical rf power and magnetic field parameters, a maximum of 30 A of continuous electron current was extracted. Figure 9 shows the extracted electron current as a function of the applied magnetic field strength for a xenon plasma using 1300 W rf power at 13.56 MHz. When the data

was collected for Fig. 9 the NES device was operated in a total nonambipolar mode where the ratio of the ion loss area to the electron loss area satisfy Eqn. 2.<sup>30</sup> A maximum of 30 A of ion current collection was extracted with a bias of -40 V on the ion collection cylinder with an applied magnetic field strength of 275 Gauss, the maximum magnetic field that could be produced with the DC power supply used for the experiment. The electron current was collected to a grounded anode and a separate current meter was used to verify the measurement of the electron current extracted by the anode. The increase in the amount of extracted electron current increases relatively linearly with the applied magnetic field strength, where the increase in magnetic field leads to an increase in the plasma density which then leads to an increase in the amount of extracted current. A saturation in the amount of extracted electron current did not occur within the current range of applied magnetic field strength (0 to 275 gauss). When NES is operated with a xenon plasma, the amount of extracted electron current, 30 A, produced by NES is more than 10 times larger than the state-of-the-art (in 2007) capabilities of existing rf plasma cathode technologies. This large increase in the current state-of-the-art should prove useful in spacecraft applications as well as in materials processing applications where high-current, steady-state, plasma-based electron sources are required.



**Figure 7. Argon and xenon plasma density as a function of the neutral gas pressure. 500 W of applied rf power at 13.56 MHz, 10 Gauss magnetic field strength**

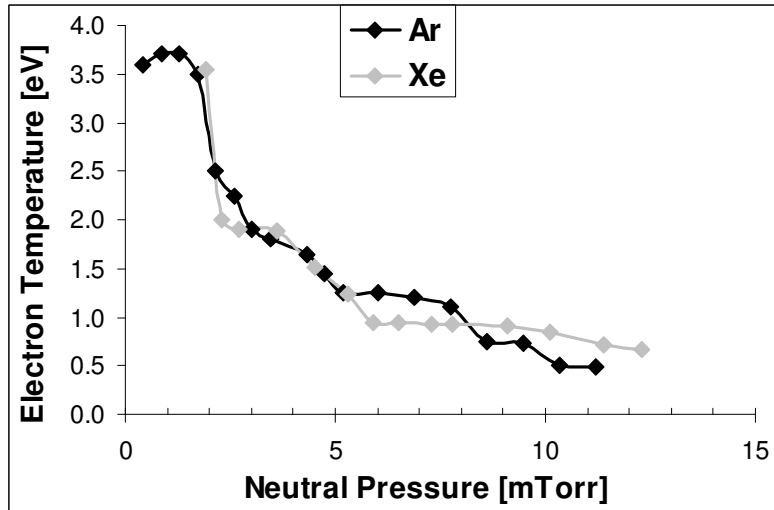


**Figure 8. Argon and xenon electron temperature as a function of the neutral gas pressure. 500 W of applied rf power at 13.56 MHz, 10 Gauss magnetic field strength.**

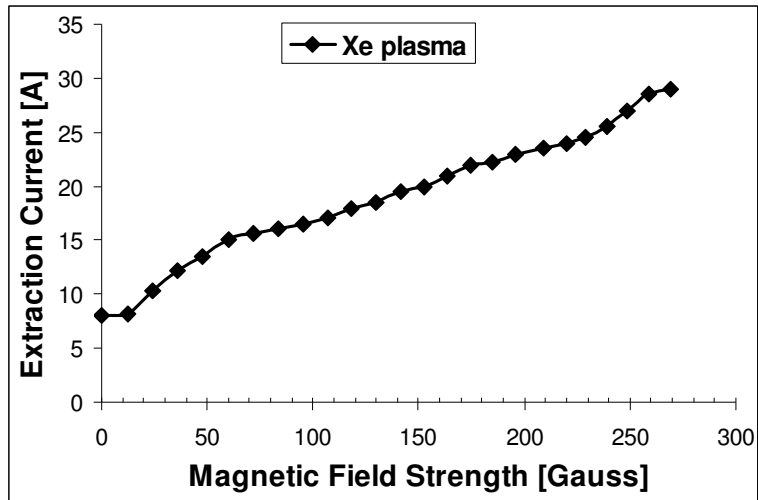


**Figure 9.** Extracted electron current as a function of the applied magnetic field strength for a Xe plasma with a flow rate of 2.2 sccm Xe, and an applied rf power level of 1300 W at 13.56 MHz.

### B. Improved Gas Utilization with Xenon

For in-space electron source applications, it is beneficial to use a plasma production method that can create the largest ionization fraction possible so that neutral gas is not expelled before it can participate in electron production. This means that an increase in plasma density for a given flow rate or internal neutral pressure results in improved performance of the electron source.

Gas utilization is defined as the ratio of electron current that is extracted to the amount of neutral particle current that flows out of the system, where 1 sccm of neutral gas flow corresponds to a particle flow or particle current of 0.072 A. In Fig. 10, the gas utilization within NES is graphed as a function of Ar flow rate for varying rf power levels. At a flow rate of 3 sccm and 1200 W rf power, a 40x gas utilization is achieved, which means that on average there are 40 electrons that exit the system for each neutral that flows through and exits the system.

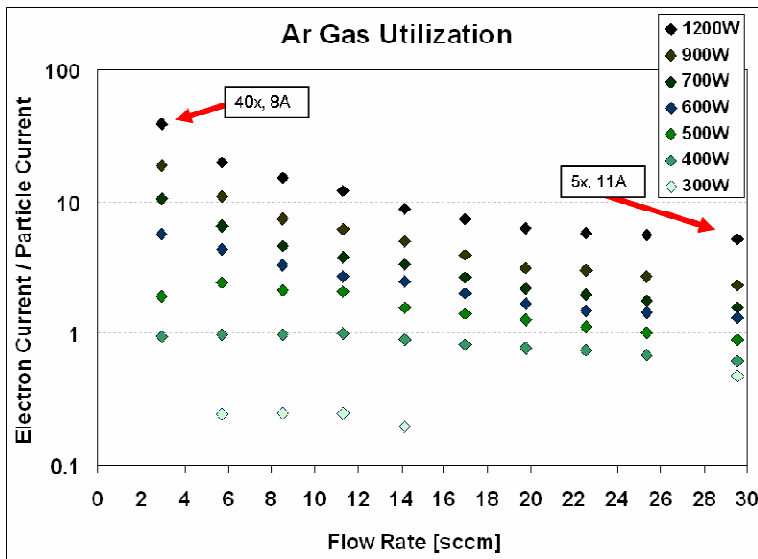


**Figure 10.** Extracted electron current divided by the neutral particle current as a function Ar flow rate for various rf power levels. A 20x gas utilization is achieved with 3 sccm Ar at 1200W rf, 100 Gauss at the exit aperture.

This is consistent with the observed data because as the applied rf power is increased from 300 W to 1200 W for the same internal neutral pressures, the plasma density increases thereby leading to an increase in the electron flux at the aperture and hence an increase in the extracted electron current and gas utilization.

As the ionization fraction increases, the argon residence time increases because the ‘average’ argon particle will spend more time as an ion. Ions are reflected at the extraction aperture within NES which leads to an improved gas utilization. As the applied rf power increases from 400 W to 1200 W for the 3 sccm case, the plasma density



increases from  $2 \times 10^{11} \text{ cm}^{-3}$  to  $2 \times 10^{12} \text{ cm}^{-3}$  and the ionization fraction increases from  $\sim 1:1000$  to  $\sim 1:100$ , leading to a gas utilization increase from 0.5 to 20.

Figure 10 also indicates that there is a maximum gas utilization that occurs for any given applied rf power level. The maximum for 300 W, 400 W, and 500 W occurs at 11 sccm, 6 sccm for 600 W and the other maximum gas utilizations occur at 3 sccm for higher power levels. Below 3 sccm, the pressure within NES was too low to sustain a plasma discharge for the  $1.23 \text{ cm}^2$  aperture.

Typical ion thrusters use xenon neutral gas as a propellant because of its larger mass and inert properties. Figure 11 shows that a Xe plasma is able to produce a significantly higher gas utilization factor than similar experiments performed with Ar plasma. Xe has an ionization potential of 12.13 eV compared to the ionization potential of 15.76 eV for  $\text{Ar}^{31}$ , making higher plasma densities possible for rf discharges such as NES.

The increase in gas utilization is due two 2 primary factors:

- 1) Xenon's neutral gas flow velocity is slower than argon's, which results in a longer residence time of xenon neutrals within the electron source.
- 2) An increase in plasma density was observed with xenon operation compared to argon operation for identical system parameters, where the amount of extracted current scales linearly with the plasma density according to Eqn. 1.

Fig. 11 does not represent the maximum gas utilization that was achieved because the DC power supply that was used to bias the ion collection cylinder was limited to 12.4 A of current, limiting the magnetic field strength to 275 Gauss. Later experiments showed (see Fig. 9) that the maximum extracted electron current was 30 A, produced using a xenon plasma and yielding a gas utilization factor of 180 at 2.2 sccm, which is 20x greater than other state-of-the-art (in 2007) rf plasma-based electron sources.

### C. Plasma Coupling Modes with Argon

A variety of rf plasma sources exist including capacitive and inductive sources, which can operate without magnetic fields, and both electron cyclotron resonance (ECR) and helicon sources, which require magnetic fields.<sup>29</sup> Helicon sources appear to be the best choice of rf plasma sources for use in high power/current ion propulsion because they have the highest ionization efficiency and can produce the highest plasma densities, up to  $10^{13} \text{ cm}^{-3}$  is common, for a given rf power. The magnetic fields that are required for ECR and helicon plasma sources can be generated by electromagnets or permanent magnets. If insufficient rf power is available, helicon sources operate as inductive sources resulting in decreased plasma densities and power efficiencies. At much lower rf power levels, the plasma is capacitively coupled with even lower plasma densities.

It has been experimentally determined that with sufficient rf power ( $>1000 \text{ W}$  at 13.56 MHz) and applied magnetic field strength ( $>70 \text{ gauss}$ ) NES is able to operate in a helicon mode with an argon feed gas. This ability for NES to operate in a helicon mode is significant in that an increased fractional ionization can be obtained compared to other coupling modes. An increased fractional ionization leads to an increased electron extraction current for similar rf power levels and an overall increase in power and gas use efficiency of the electron source.

A Faraday shield is used in the NES device to reduce capacitive coupling. If the Faraday shield is removed from the plasma column, a large fluctuating plasma potential of over 200 V peak-to-peak is observed. In an inductive mode the plasma potential fluctuations are present to a substantial degree and are measured to be in excess of 100 V p-p.

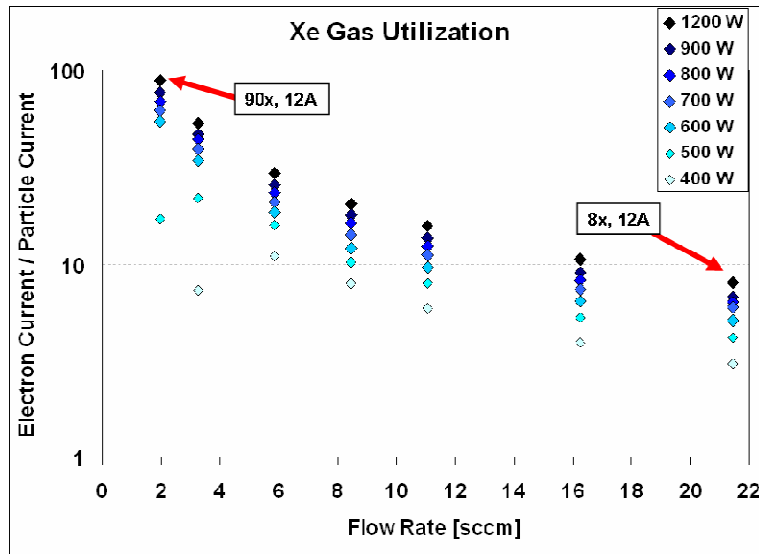


**Figure 11. Extracted electron current divided by the neutral particle current as a function of neutral Xe flow rate for various rf power levels. A 90x gas utilization is achieved with 2.2 sccm Xe at 1200W rf, 100 Gauss at the exit aperture.**

When the Faraday shield was used, the fluctuations in the plasma potential were reduced to less than 0.5 V peak to peak.

If capacitive coupling to the plasma is reduced, then the dominant coupling mode will be inductive coupling for low rf power levels and low magnetic field levels. A magnetic field is not necessary to inductively couple to the plasma, however it was previously demonstrated that the presence of a 100 Gauss magnetic field could significantly increase the plasma density and reduce the fraction of electron current that was parasitically drawn to the electron extraction ring.<sup>30</sup>

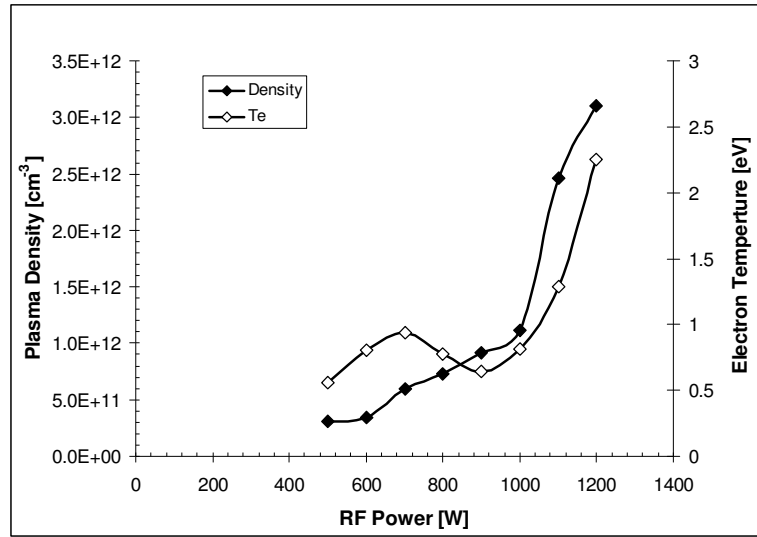
If a combination of sufficient rf power and magnetic field strength exists, the rf antenna can inductively couple to the plasma in a helicon mode. Helicon mode coupling is characterized by increased plasma densities and highly efficient ionization compared to capacitively and inductively coupled plasmas.<sup>29</sup> The presence of a helicon mode transition was investigated by looking at the plasma density, electron temperature, and plasma spectral lines as a function of the applied rf power level.

Figure 12 shows double probe measurements of the plasma density and electron temperature within NES as a function of the applied rf power. A flow rate of 15 sccm Ar was used with a 70 Gauss magnetic field, and an ion collection cylinder bias of -50 V.

A clear helicon mode transition occurs when the applied rf power is increased from 1000 W to 1100 as both the electron temperature and the plasma density increase sharply at that point. The sharp increase in plasma density over a narrow range of rf power is associated with a mode change<sup>29</sup>, in this case from an inductive mode to a helicon mode. A transition from capacitive mode to inductive mode is not observed because of the effectiveness of the Faraday shield at blocking the capacitive coupling to the plasma. Conventional inductive and helicon plasma sources are ignited through an initial capacitive mode coupling, however because this mode is purposely blocked, a Tesla coil is applied between the extraction ring and the grounded anode in order to initiate the discharge.

The floating potential on a single conducting tip probe was also measured on an oscilloscope as a function of time. The floating potential oscillates back and forth at a frequency of 13.56 MHz (the driving frequency). The peak to peak floating potential fluctuations also support a transition from an inductive mode to a helicon mode as the fluctuations drop significantly near an rf power level of 1000 W, as seen in Fig. 13.

Spectral data were also taken in order to look for an inductive to helicon mode transition at higher applied power levels for a fixed magnetic field level of 100 gauss. Figure 14 shows two spectral samples taken for applied rf power levels of 500W and 1200 W. The 400 W data show spectral peaks that correspond to neutral Ar atom (Ar I) transitions. The 1200 W data show spectral peaks from similar Ar I transitions, but also show two transitions for Ar II, singly ionized argon ions.<sup>31</sup> As the applied rf power is increased from 400 W (light gray)



**Figure 12. Ar plasma density and electron temperature double probe measurements as a function of the applied rf power.**

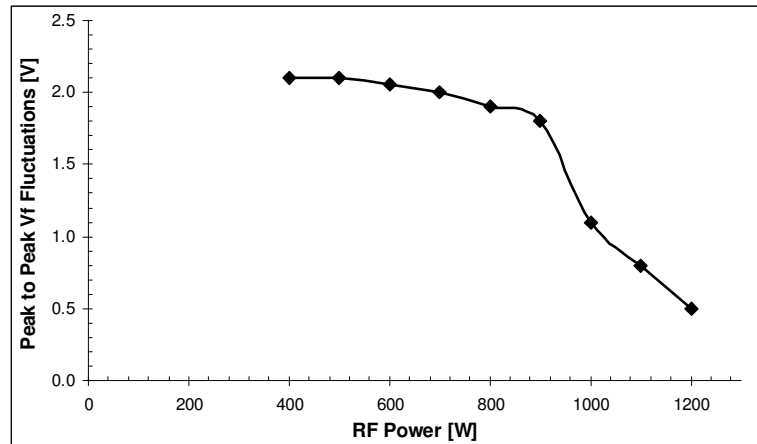


**Figure 13 Floating potential fluctuations as a function of the applied rf power using 15 sccm Ar, -50 ion cylinder bias, 70 gauss magnetic field.**

to 1200 W (dark gray), two peaks centered on two ArII emission lines (indicated by an arrow) are observed, indicating a significant increase in the fractional ionization of the neutral particles, which is associated with a helicon mode transition.

The four sets of data, electron temperature, plasma density, peak-to-peak potential fluctuations, and optical transitions, presented in this section provide a consistent picture of an inductive mode to helicon mode transition. This ability for NES to operate in a helicon mode is significant in that an increased fractional ionization can be obtained which leads to an increased electron extraction current for similar rf power levels and an overall increase in power and gas utilization efficiency for the electron source.

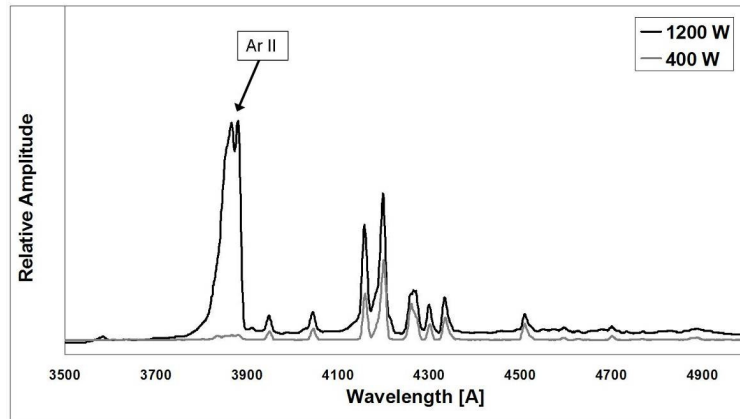


**Figure 14.** Spectral data from 350 nm to 500 nm, for 400 W (light gray) and 1200 W (dark gray) applied rf power levels.

#### IV. Conclusion

An electron sheath allows for the extraction of all the random electron flux through an exit aperture that is a factor of  $\sqrt{2m_i/\pi m_e}$  smaller (230 for argon, 410 for xenon) than the ion loss area located within the plasma source. The Nonambipolar Electron Source (NES) has generated 30 A of electron current that could be used for the purposes of plasma generation or neutralization in a Hall or gridded ion thrusters. 30 A of extracted current was achieved using 2.2 sccm Xe, 1300 W of rf power at 13.56 MHz, 275 gauss at the exit aperture, and a -40 V DC bias on the ion collection cylinder. The ion collection cylinder, with an area of 590 cm<sup>2</sup>, provided the necessary ion loss area, while a smaller grounded ring was used to extract the electrons through an electron sheath into the target region of the plasma chamber. An axially symmetric DC magnetic field created a uniform plasma potential across the exit aperture of NES which allowed for the extraction of all the incident electron flux through an electron sheath. A unique feature of this proof of principle gridded electron source is the total non-ambipolar extraction of electrons through an electron sheath, where all of the electrons in the system were extracted by the electron sheath at the exit aperture and all of the ions in the system were lost at the ion sheath at the chamber walls of NES.

By operating with a Xe neutral gas, a higher plasma density is achievable which ultimately leads increases in total electron current output and increase in the energy efficiency of the device.

Helicon mode operation was experimentally verified within the NES device for an argon plasma. Changes in electron temperature, plasma density, peak-to-peak potential fluctuations, and optical spectra measurements taken within NES all provide a consistent picture of an inductive mode to helicon mode transition at 1000 W rf power and 100 gauss magnetic field. This ability for NES to operate in a helicon mode is significant in that an increased fractional ionization and plasma density results in an increased electron extraction current for similar rf power levels and an overall increase in power and gas utilization efficiency for the electron source.

Because NES generates a high density plasma from an rf power source and does not rely on material cathodes for the production of electrons it could be useful as an electron source for long duration space exploration and cargo missions using ion propulsion and may permit for missions that were previously unfeasible with conventional electron sources.

#### Acknowledgments

The research described in this paper was carried out at the University of Wisconsin – Madison, under an STTR grant with the National Aeronautics and Space Administration and was also supported in-part by the Wisconsin Space Grant Consortium (B.L.).

## References

- <sup>1</sup>Morgner, H., Neumann, M., Straach, S., Krug, M., Surf. Coat. Technol. 108 (1), 513-519 (1998).
- <sup>2</sup>Singh, B., Mesker, O.R., Levine, A.W., Aire, Y., Appl.Phys.Lett. 52 (20), 1658-1660 (2006).
- <sup>3</sup>Chou,W.J., Yu, G.P., Huang, J.H., Surf. Coat. Technol. 149 (1), 7-13 (2002).
- <sup>4</sup>Williams, D.G. J. of Vac. Sci. and Technol. 11, 374 (1974).
- <sup>5</sup>Hellmich, A, T. Jung, A. Keilhorn, M. Riszland, Surf. Coat. Technol. 98 (1), 1541-1546 (1998).
- <sup>6</sup>Goebel,D., Katz, I., Polk, J., Mikellides, I.G., Jameson, K.K., Liu, T., Doughery, R., Proceedings of the AIAA Space 2004 Conference and Exposition, San Diego, CA, September 28-30, 2004. pp. 841-852.
- <sup>7</sup>Oleson, S., Proceedings of the 40th Joint Propulsion Conference and Exhibit, Fort Lauderdale, FL, July 11- 14, 2004, AIAA-2004-3449.
- <sup>8</sup>Sengupta, A., Brophy, J.R., Goodfellow, K.D., Proceedings of the 39th Joint Propulsion Conference and Exhibit, Huntsville, AL, July 20-23, 2003, AIAA 03-4558.
- <sup>9</sup>Sarver-Verhey, T., Proceedings of the 26th International Electric Propulsion Conference, Kitakyushu, Japan, October 17-21, 1999, IEPC-99-126.
- <sup>10</sup>Kaufman, H., Robinson, R., U.S. Patent No. 4,954,751 (4 September, 1990).
- <sup>11</sup>Jahn, R.G., in *Physics of Electric Propulsion*, (Dover Publications, New York, 2006), pp. 304-313.
- <sup>12</sup>Chen, F.F., in *High Density Plasma Sources*, edited by O. A. Popov, (Noyes Publications, Park Ridge, NJ, 1995), Chap. 1, pp. 5-61; J. E Stevens, *ibid.*, Chap. 7, pp. 312-355.
- <sup>13</sup>Gilland, J., Breun, R., Hershkowitz, N., Plasma Sources Sci. Technol. 7 (3), 416-22 (1998).
- <sup>14</sup>Kuninaka, H., Nishiyama, K., Shimizu, Y., Toki, K., Proceedings of the 40th Joint Propulsion Conference and Exhibit, Ft. Lauderdale, FL, July 11-14, 2004, AIAA-2004-3438.
- <sup>15</sup>Foster, J.E., Kamhawi, H., Haag, T. Carpenter, C., Williams, G.W., National Aeronautics and Space Administration Report, NASA/TM-2006-214035 (2006).
- <sup>16</sup>Diamant, K.D., Proceedings of the 41st Joint Propulsion Conference and Exhibit, Tucson, AZ, July 10-13, 2005, AIAA-2005-3662.
- <sup>17</sup>Diamant,K.D., Proceedings of the 42nd Joint Propulsion Conference and Exhibit, Sacramento, CA, July 9-12, 2006, AIAA-2006-5154.
- <sup>18</sup>Korzec, D., Müller, A., Engemann, J., Rev. Sci. Instrum. 71, 800 (2000).
- <sup>19</sup>Severn, G.D., Hershkowitz, N., Phys. Fluids B 4 (10), 3210 (1992).
- <sup>20</sup>Longmier, B., Hershkowitz, N., "'Electrodeless" Plasma Cathode for Neutralization of Ion Thrusters," 41<sup>st</sup> AIAA/ASME/SAE/ASEE Joint Propulsion Conference & Exhibit , 1-7, 2005.
- <sup>21</sup>Longmier, B., Hershkowitz, N., "Nonambipolar Electron Source for Neutralization of Ion and Hall Thrusters," IEPC-2005-301 , 1-7, 2005.
- <sup>22</sup>Elliott, F.W., Foster, J.E., and Patterson, M.J., "An Overview of the High Power Electric Propulsion (HiPEP) Project," AIAA-2004-3453, 40th AIAA/ASME/SAE/ASEE Joint Propulsion Conference & Exhibit 11- 14 July 2004, Fort Lauderdale, FL.

<sup>23</sup>Funaki, I., Kuninaka, H., "Overdense Plasma Production in a Low-power Microwave Discharge Electron Source," Jpn.J.Appl.Phys 40, 2495-2500, 2001.

<sup>24</sup>HACK, K.J., et al., "Evolutionary use of nuclear electric propulsion," AIAA, Space Programs and Technologies Conference, Huntsville, AL, 1990.

<sup>25</sup>HACK, K.J., GEORGE, J.A., DUDZINSKI, L.A., "Nuclear electric propulsion mission performance for fast piloted Mars missions," AIAA, NASA, and OAI, Conference on Advanced SEI Technologies, Cleveland, OH , 1991.

<sup>26</sup>Gilland, J.H., "Mission and System Optimization of Nuclear Electric Propulsion Vehicles for Lunar and Mars Missions," Springfield, Va.: National Aeronautics and Space Administration; National Technical Information Service, distributor, 1991.

<sup>27</sup>Godyak, V.A., Piejak, R.B., Alexandrovich, B.M., "Electron-energy distribution function in a shielded argon radiofrequency inductive discharge," Plasma Sources Sci.Technol. 4 (3), 332, 1995.

<sup>28</sup>Hershkowitz, N., "How Langmuir Probes Work," Plasma Diagnostics , 113-83, 1989.

<sup>29</sup>Chen, F.F., in 37th Annual Meeting of the Division of Plasma Physics of the American Physical Society, 6-10 Nov. 1995, AIP, Louisville, KY, USA, pp. 1783-93.

<sup>30</sup>Longmier, B., Hershkowitz, N., "Nonambipolar Electron Source," Rev. Sci. Instrum. 77, 113504, 2007.

<sup>31</sup>Lide, D.R., CRC Handbook of Chemistry and Physics, 2000-2001, edited by Anonymous 80th ed. (CRC Press Boca Raton, 2000).